Title:

Remote Cortical Network for Frontal Cognitive Symptoms derived from Tau Accumulation in Progressive Supranuclear Palsy

Authors:

Yuki Hori[a], Hironobu Endo[a*], Kenji Tagai[a], Yuko Kataoka[a], Ryoji Goto[a], Shin Kurose[a], Yuki Momota[a], Naomi Kokubo[a], Chie Seki[a], Sho Moriguchi[a], Hitoshi Shimada[a,b], Hitoshi Shinotoh[a], Takahiko Tokuda[a], Keisuke Takahata[a], Takafumi Minamimoto[a], Makoto Higuchi[a,c], and Toshiyuki Hirabayashi[a*]

Affiliations:

[a] Advanced Neuroimaging Center, National Institutes for Quantum Science and Technology, 4-9-1 Anagawa, Inage-ku, Chiba 263-8555, Japan

[b] Center for Integrated Human Brain Science, Department of Functional Neurology & Neurosurgery, Niigata University, 1-757 Asahimachidori, Chuo-ku, Niigata 951-8585 Japan

[c] Department of Neuroetiology and Diagnostic Science, Osaka Metropolitan University Graduate School of Medicine, Osaka 545-8585, Japan

[*] Authors to whom all correspondence should be addressed:

Toshiyuki Hirabayashi, Ph.D.

Advanced Neuroimaging Center, National Institutes for Quantum Science and Technology, 4-9-1 Anagawa, Inage-ku, Chiba 263-8555, Japan

E-mail: hirabayashi.toshiyuki@qst.go.jp

Hironobu Endo, M.D. Ph.D.

Advanced Neuroimaging Center, National Institutes for Quantum Science and Technology, 4-9-1 Anagawa, Inage-ku, Chiba 263-8555, Japan

E-mail: endo.hironobu@qst.go.jp

Abstract:
Progressive Supranuclear Palsy (PSP) is a neurodegenerative disorder characterized by impaired movement and frontal cognitive dysfunction. While motor symptoms have been linked with subcortical tau deposits, mechanisms underlying the frontal cognitive symptoms remain unclear because pathological tau accumulation is quite limited within the frontal cortex and heterogeneously distributed primarily in the subcortical regions. Here, we combined high-contrast tau-PET with normative connectome to resolve this issue. Tau-deposition sites were found to be connected to a common cortical network that was not detectable through atrophy-based analyses. This network was primarily overlapped with canonical action-mode and frontoparietal networks. While the degree of subcortical primary tau deposition or atrophy correlated with motor symptoms, only connectivity from tau-deposition sites to the derived cortical network explained the frontal cognitive deficits. These findings suggest that frontal cognitive impairments in PSP are derived from remote effects of tau deposits, independent of atrophy, through the identified common cortical network.

Main Text:

INTRODUCTION

Progressive supranuclear palsy (PSP) is a neurodegenerative disorder primarily characterized by movement impairments such as oculomotor deficits, postural instability, and akinesia[1-3]. In addition to these motor-related symptoms, PSP is frequently associated with cognitive deficits, especially those related to frontal cortical function[4,5]. Pathologically, PSP is known as a four-repeat tauopathy, where the aggregation of hyperphosphorylated tau proteins is implicated as a major cause of clinical symptoms, accompanied by neuroinflammation and atrophy[6,7]. Tau lesions, neuronal loss, and gliosis have been found primarily in subcortical regions, and in a part of cortical regions, including the basal ganglia, midbrain, motor-related cortical areas, and cerebellum[8], and damage to these structures has been associated with motor dysfunction and general disease severity[2,3,9,10]. Subcortical atrophy—especially in the midbrain and cerebellum—is another notable pathological hallmark of PSP, and can be used to distinguish patients with PSP from those with Parkinson's disease or age-matched healthy controls[11,12]. However, the mechanisms underlying the frontal cognitive decline in PSP remain elusive, as frontal lobe atrophy or tau deposition is rarely observed beyond the primary and supplementary motor areas [12-15].

Neurodegenerative diseases, including PSP, are increasingly being conceptualized as network-based disorders[16]. The aggregation of pathological proteins in specific brain regions disrupts synaptic function, with damage propagating across interconnected networks[17,18], and accelerating clinical symptoms[19]. In PSP, reduced functional connectivity (FC) between the atrophied midbrain region and other areas including the frontal cortex has been reported[20]. In addition, hypoperfusion[21,22] and hypometabolism[23,24] in the frontal cortex have been observed even in the absence of local pathological changes, suggesting that the frontal cognitive dysfunctions in PSP might result from the remote effects of subcortical pathology.

Using normative connectome data, lesion network mapping (LNM) is a powerful approach for identifying brain regions commonly connected to heterogeneous lesion sites that are associated with shared symptoms across patients with stroke. This approach is based on the principle that in addition to direct local impairments, a lesion in a given brain region also indirectly impairs functions governed by remote regions connected from the lesion site. LNM has uncovered hidden core regions associated with diverse symptoms across neurological conditions, including visual hallucinations[25], delusional misidentifications[26], amnesia[27], loss of consciousness[28], criminal behavior[29], and abnormal movements such as freezing of gait and hemichorea-hemiballismus[30]. Recently,

LNM has been extended to atrophy-based analyses in Alzheimer's disease[31], demonstrating its potential for identifying common brain locations functionally connected with atrophied regions, despite the large individual variation in atrophy patterns across patients. Importantly, core regions identified through LNM have been shown to align with previously identified neuromodulatory targets for symptom relief[32,33], further validating its utility. Network mapping based on tau deposits was conducted in a recent paper with cohorts of Alzhimer's disease[34]. However, critical comparisons between the influences of local tau deposits and their remote effects on a specific symptom, between the effects of tau deposits and atrophy on the network mapping, or between the effects of tau deposits and random control seeds on the network mapping have not been conducted yet.

In the current study, we hypothesized that a common network extended from tau deposition is responsible for the frontal cognitive dysfunction observed in PSP. Specifically, we investigated whether motor and frontal cognitive impairments in PSP could be attributed to local tau deposition or atrophy, or to their remote effects. After finding evidence for this, we sought to determine whether the remote effects are specific for frontal cognitive dysfunction and whether they differ from those of atrophy. To achieve this we used florzolotau (18F) (also known as PM-PBB3 or APN-1607), a novel PET probe that we recently developed for detecting tau deposits[35]. This probe provides high metabolic stability and remarkable contrast at the single-patient level not only for Alzheimer's disease (AD), but also for non-AD tauopathies including PSP, which has been difficult with previous probes[36]. By applying network mapping to PET-detected tau deposits in individual patients, we identified common brain regions that are functionally connected from the locations of pathological tau aggregates, and examined their relationships with clinical symptoms (Fig. 1). Our results indicate that a network mechanism underlies the frontal cognitive impairments in PSP and highlight the distinct contribution of remote effects mediated by tau deposits.

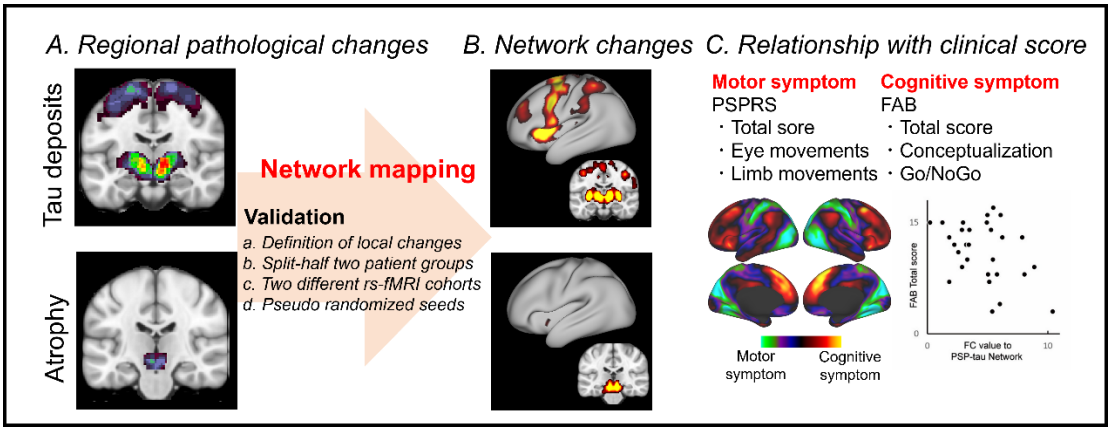

Figure 1 **Overview**. Identification of the regional and network impairments responsible for the frontal cognitive dysfunction in progressive supranuclear palsy. **(A)** Regional impairments caused by tau deposits and atrophy were identified by ^{18}F-florzolotau PET and MRI, respectively. **(B)** Network impairments were identified using a resting-state functional MRI (rs-fMRI) database of healthy participants and regional impairments as seeds. **(C)** Finally, the relationship between clinical symptoms and a specific brain region or functional network was determined.

RESULTS

Localization of tau deposits and brain atrophy in individual patients with PSP

We analyzed the data from 37 patients (22 males and 15 females) with PSP-Richardson syndrome, which presents the most typical clinical features of PSP[37]. The mean patient age and disease duration were 70 ± 1.2 years and 3.4 ± 0.40 years (mean ± SEM, respectively. Disease severity as assessed by the PSP rating scale (PSPRS) was 41 ± 2.9. All patients exhibited tau deposits visualized and quantified with florzolotau PET, without any accumulation of amyloid-beta, as determined by Pittsburgh compound-B (PiB) PET.

To identify the locations of tau deposition and atrophy, we first calculated *t*-score maps of florzolotau PET and MRI-based voxel-based morphometry (VBM) images for each patient. These maps were generated by comparing patient data with the corresponding images of age-matched healthy controls (N = 48) (Fig. 2). Across patients, tau deposits were most frequently observed subcortically in the globus pallidus (GP) ($p < 0.0003$, unpaired *t*-test) and midbrain ($p < 0.0006$), with 62% and 57% overlaps across patients when thresholded at $p = 0.001$, respectively (Fig. S1C). In addition, moderate tau accumulation was also detected in motor-related cortical areas in the precentral gyrus ($p < 0.003$, 25% overlap). Meanwhile, brain atrophy was primarily localized to the midbrain ($p < 0.01$, 27% overlap), cerebellum ($p < 0.03$, 27%), and GP ($p < 0.05$, 14%) (Fig. S1B and D). Note that overlap of both tau deposition and atrophy was extremely limited in the frontal cortex, except for parts of the primary/supplementary motor and premotor areas.

Common extended network derived from tau deposits or brain atrophy across patients with PSP

Next, we sought to determine whether common networks functionally connected to tau deposits and/or atrophy locations could be observed in the patients. We first examined the brain regions that were functionally connected to the tau deposit locations in each patient using a tau-network mapping approach (See Fig. S2). The locations of tau deposit in each patient were identified based on the *t*-score map ($p < 0.001$, one-sided, uncorrected). These locations then served as seed regions for calculating the whole-brain FC maps using a publicly available resting-state functional MRI (rs-fMRI) dataset of healthy subjects [Brain Genomics Superstruct Project (GSP)[38]] (N = 100)[25]. Although tau deposits were restricted to subcortical areas and some portions of motor-related cortex (Fig. 2A and C), the analysis revealed a common network derived from tau deposits that extended to widespread cortical areas, including the lateral prefrontal cortex (LPFC), dorsal anterior cingulate cortex (dACC), posterior parietal cortex (PPC), anterior insula (AI) ($p < 0.05$, family-wise error (FWE)-corrected; Fig. 3A and D). In contrast, atrophy network

mapping—with thresholded ($p < 0.001$, uncorrected) atrophy maps from the same patients as seed regions—revealed an extended network largely restricted to subcortical areas, including the midbrain, pons, and a part of cerebellum (Fig. 3B and E). These results suggest that the extended, common cortical network observed in the patients is derived specifically from tau deposits, rather than atrophy.

To validate these results, we conducted several control analyses. First, we confirmed that the observed common network was basically conserved even when different thresholds ($p < 0.005$, uncorrected or $p < 0.05$, FWE corrected) were used to define the seed regions from the tau-accumulation (Fig. S3A-F) and atrophy (Fig. S3G-L) maps, suggesting that the results did not depend on a specific threshold value for seed definition. Second, the reproducibility of the common cortical network was assessed by splitting the original dataset into two random subgroups. The resultant FC maps derived from tau deposits or atrophy were significantly correlated between the two subgroups (Fig. S4, $r =$ 0.87 and 0.74, $p < 0.001$ for tau- and atrophy-network mapping, respectively). Third, to rule out connectome-specific effects, we calculated the tau deposit-derived network using an alternative publicly available rs-fMRI database [human connectome project (HCP)][39] . The cortical nodes identified in this analysis were similar to those derived using the GSP database (Fig. S5), supporting the robustness of our findings across different rs-fMRI datasets. Lastly, to ensure that the resultant networks were specific to the tau-deposit or atrophy locations, and not merely a reflection of hub regions in the brain, we contrasted the tau- and atrophy-network maps against corresponding control maps generated with spatially randomized seed regions. The results were consistent with the original tau- and atrophy-network maps, confirming that the observed common networks were specifically derived from tau-deposit and atrophy locations in patients with PSP (Fig. S6).

Because tau deposits are thought to cause neuronal loss and subsequent atrophy[6], one possible concern is that the observed tau deposit-derived network might partially reflect the remote effects of atrophy. To isolate the tau-specific extended network, we further contrasted the tau- and atrophy-derived network maps. This analysis revealed cortical nodes with significantly stronger connectivity from the tau-deposit locations than from the atrophy locations, including the anterior dorsolateral PFC (adlPFC), pre-supplementary motor area (pre-SMA), dACC, premotor cortex (PMC), inferior frontal cortex (IFC), AI, and PPC ($p < 0.05$, FWE-corrected; Fig. 3C and F). Importantly, no regions showed the opposite pattern (i.e., significantly stronger connectivity from the atrophy locations than from the tau-deposit locations). We refer to the cortical network derived specifically from tau deposits as the PSP-tau network.

To assess whether the derived PSP-tau network corresponds to specific canonical functional networks in healthy individuals, we mapped the regions in the PSP-tau network onto 12 functional networks defined in Ji et al[40] (Fig. 3G). The distribution of regions across the networks were significantly uneven ($p < 1.0\times10^{-16}$, Chi-squared test), with the majority of regions assigned to the cingulo-opercular (action-mode)[41] network (CON: 66%), followed by the frontoparietal (FPN, 29%), and language (LAN, 5.3%) networks. No nodes from any of the other nine networks (orbito-affective, ventral multimodal, posterior multimodal, default mode, auditory, dorsal attention, somatomotor, primary visual, and secondary visual networks) were included in the PSP-tau network (Fig. 3H). These results suggest that the cortical remote dysfunction caused predominantly by subcortical tau deposition in patients with PSP is primarily linked to specific networks, especially CON and FPN.

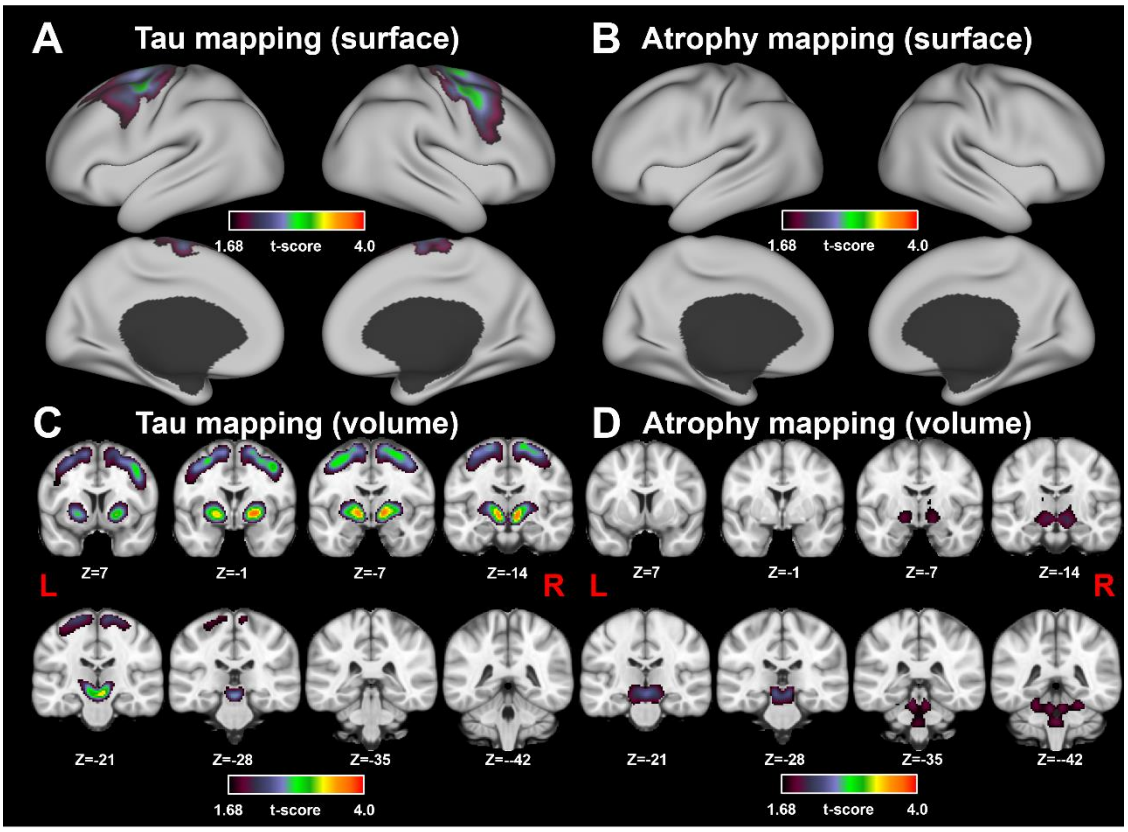

Fig. 2 **Population maps for tau deposition and atrophy among patients with progressive supranuclear palsy**. **(A-B)** Mean *t*-score maps of tau deposition (A, C) and atrophy (B, D) among PSP patients were presented on the surface (A, B) and volume space (C, D). Tau deposits were primarily observed subcortically in the globus pallidus and midbrain. Moderate accumulation of tau was also detected in motor-related cortical areas in the precentral gyrus. Brain atrophy was observed in the midbrain and cerebellum. *t*-scores derived from an unpaired *t*-test conducted against healthy controls. Brain atrophy was observed in midbrain and cerebellum. Unpaired *t*-test was conducted against healthy controls.

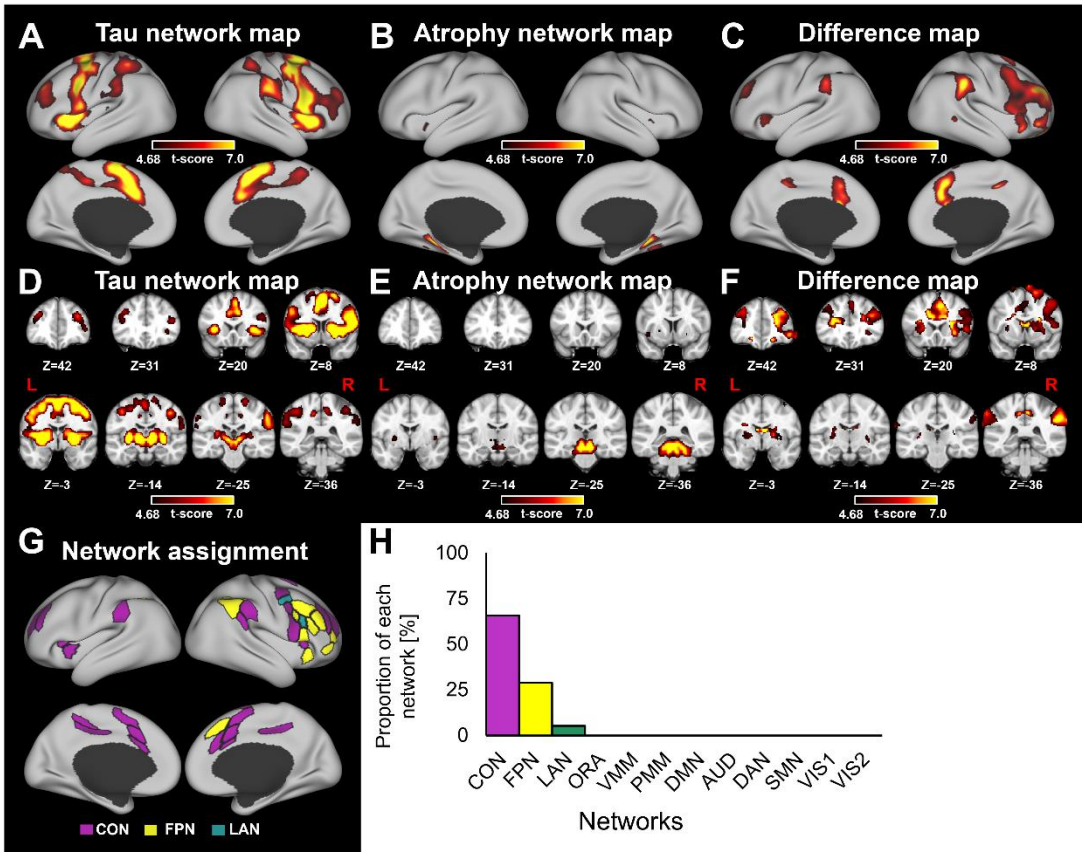

Fig. 3 **Tau- and atrophy-network maps for patients with progressive supranuclear palsy**. **(A-F)** Average network maps calculated using tau deposit and atrophy VOIs among patients were presented on the surface (A and B for tau and atrophy, respectively) and volume space (D and E for tau and atrophy, respectively). *t*-score maps were obtained by comparing functional connectivity maps of tau deposit seeds vs. atrophy seeds (C and F). **(G-H)** Overlap with known functional networks. Based on the cortical parcellation created by Ji et al. (2019), one of twelve networks was assigned to each region in the difference map (G), and the proportion of each network area to the total area (38 areas) was calculated (H). *CON*: Cingulo-opercular network; *FPN*:

Frontoparietal network; *LAN*: Language network; *ORA*: Orbito-affective network; *VMM*: Ventral multimodal network; *PMM*: Posterior multimodal network; *DMN*: Default mode network; *AUD*: Auditory network; *DAN*: Dorsal attention network; *SMN*: Somatomotor network; *VIS1*: Visual network 1; *VIS2*: Visual network 2.

FC between the tau-deposit locations and the PSP-tau network explained individual variability in frontal cognitive decline

To examine how the PSP-tau network relates to specific clinical symptoms at the single-patient level, we looked at the relationship between the FC from tau deposition sites to the PSP-tau network regions and clinical scores in the same patients. As a control analysis, we first examined the correlation between clinical scores and the degree of tau deposit/atrophy in the respective top two representative regions. The total score of the PSPRS correlated significantly with the degree of atrophy both in the midbrain ($p < 0.03$) and cerebellum ($p < 0.05$), but not to the amount of tau deposited in either the GP or the midbrain (Fig. 4A-B). Among the PSPRS sub-scores, the degree of eye-movement deficit significantly correlated with the amount of tau deposited in the GP ($p < 0.006$) and midbrain ($p < 0.05$) (Fig. 4A), while the degree of limb-movement deficit correlated with the amount of atrophy in the midbrain ($p < 0.04$) (Fig. 4B). However, neither the degree of tau accumulation nor the amount of atrophy significantly explained the variance in Frontal Assessment Battery (FAB) score[4], a general clinical test for measuring cognitive functions of the frontal cortex (Fig. 4A and B).

In contrast, the FC value between tau-deposit locations and the PSP-tau network significantly anti-correlated with the FAB score ($p < 0.04$), but not with any of the motor-related clinical scores ($p > 0.9$). Meanwhile, neither the FC value nor the degree of tau accumulation/atrophy significantly explained the variance in more general cognitive abilities (Mini-Mental State Examination [MMSE]; $p > 0.1$), apathy (Apathy Scale, $p > 0.3$), or depression (Geriatric Depression Score [GDS], $p > 0.1$]. To map the regions whose FC with the tau-deposit locations predominantly explained the frontal cognitive impairments compared to the motor symptoms among the whole brain, we created a map that contrasted the FC value–frontal cognitive score correlations with the FC value–motor score correlations (Fig. 4D). After calculating correlation maps using the total FAB score and sub-scores for frontal cognitive impairments, and total PSPRS score and sub-scores for motor impairments, the scores that were the best explained by the FC value were adopted for each of the frontal cognitive and motor symptoms. As a result, the total FAB score, and the PSPRS sub-score for limb movement deficit were used as indices for frontal cognitive and motor impairments, respectively. The brain areas whose degree of FC with the tau-deposit locations predominantly explained the frontal cognitive deficits were the

adlPFC, dACC, premotor cortex, IFC, AI, and PPC (Fig. 4D), all of which were consistent with the PSP-tau network (Fig. 4F: same as Fig. 3C).

More specifically, sub-scores of conceptualization and Go/NoGo in the FAB significantly anti-correlated with the FC between the tau-deposit locations and the PSP-tau network ($p < 0.005$ and $p < 0.04$ for conceptualization and Go/NoGo, respectively) (Fig. 4C). In the PSP-tau network, FC value with the Pre-SMA best explained the individual variation in total FAB score ($p < 0.007$), while that with the AI was the worst ($p > 0.1$) (Fig. S7). To visualize the most relevant clinical score for each area in the PSP-tau network, we created a clinical score map by assigning the score showing the highest positive or negative correlation with the FC values (Fig. 4G) [Correlation maps between the FC value and each of the six clinical scores (PSPRS: total score, eye-movement, limb-movement; FAB: total score, conceptualization, Go/NoGo) are presented in Supplemental Figure S8]. Over 80% of the areas in the PSP-tau network exhibited the highest correlations with the FAB-related cognitive scores. Together, these results suggest that at the single-patient level, while the motor symptoms result directly from the local effects of subcortical tau deposits or atrophy, the frontal cognitive symptoms can be best explained by a remote effect that tau deposits exerts on the PSP-tau network.

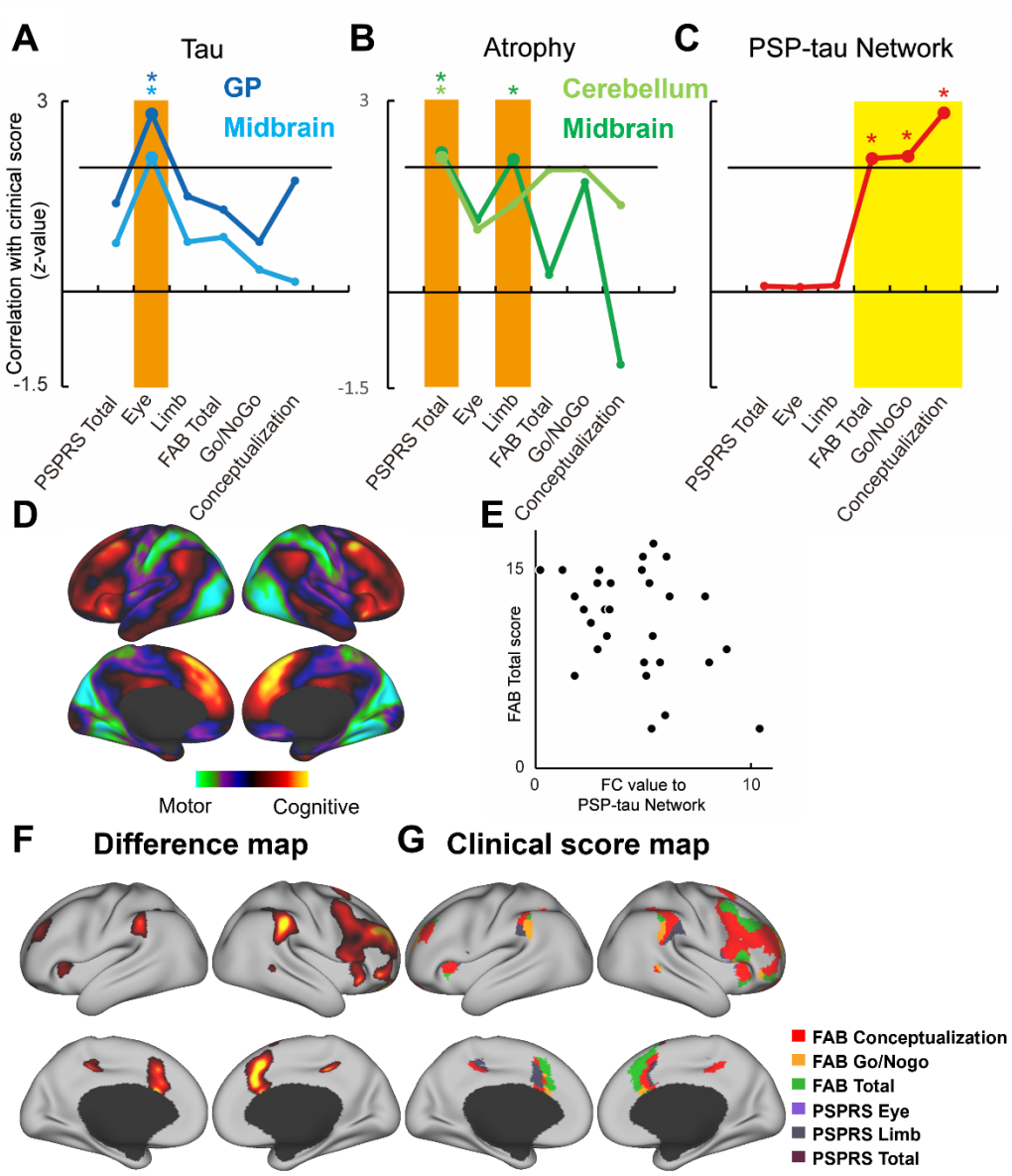

Fig. 4 **FC between the tau-deposit locations and the PSP-tau network explained individual variability in frontal cognitive decline**. **(A-B)** Correlations between motor/cognitive clinical scores and the degree of tau deposit (A)/atrophy (B) in the top two regions. Black horizontal line, statistical threshold (p = 0.05). Orange and yellow boxes with asterisk, significant correlation for motor and cognitive clinical scores, respectively. Dark and light blue in (A), the degree of tau deposit in the GP and midbrain, respectively. Dark and light green in (B), the degree of atrophy in the midbrain and cerebellum, respectively. **(C)** Correlations between clinical scores and the FC value from the tau deposits to the PSP-tau network. **(D)** Brain maps showing the regions having FC values explaining motor (PSPRS limb) or frontal cognitive (total FAB score) dysfunction. **(E)** Scatter plot showing that the FC value between the tau deposits and the PSP-tau network was negatively correlated with the total FAB score.

(F-G) The clinical scores with the strongest correlations were assigned to the brain regions that were identified as differing significantly between tau and atrophy network mapping (F, same as Fig. 3C) using a winner-take-all method (G).

DISCUSSION

Here, we conducted tau/atrophy-network mapping for PSP patients based on their tau deposits and atrophy mapped by multimodal imaging with a tau PET using a recently developed high-contrast tracer florzolotau and structural MRI. While tau deposits and atrophy were primarily detected in subcortical regions, the derived PSP-tau network was predominantly distributed across the canonical cortical networks of CON and FPN. This PSP-tau network was derived specifically from the tau deposition sites, not from regions with atrophy. Critically, while individual variation in motor symptoms was significantly explained directly by local effects of tau deposits or atrophy in subcortical regions, the frontal cognitive symptoms were significantly explained only by the remote effects of the tau deposits exerted on the cortical PSP-tau network. These results suggest that the effects of tau deposits in heterogeneous regions across the patients with PSP remotely converge onto the PSP-tau network, and this cortical convergence is why these patients exhibit their characteristic frontal cognitive symptoms, which could not be explained by local effects of tau deposits or atrophy.

Network mapping with normative rs-fMRI data from a large population of healthy individuals has been extensively conducted for brain lesions especially from stroke patients[42]. The present results demonstrate for the first time that this approach can be effectively extended to PET-detectable tau deposits in neurodegenerative disease patients, with direct comparisons with the effects of atrophy and random control seeds on the network mapping and comparisons between the influences of local tau deposits and their remote effects on specific symptoms. In particular, frontal cognitive symptoms, but not motor symptoms, in patients with PSP could be explained by the FC strength between the tau-deposition sites and the derived PSP-tau network, a proxy for the degree to which tau deposits affect these remote regions. In contrast, the amount of locally deposited tau or atrophy in subcortical regions with the maximum overlap across patients could only predict motor deficits. These results demonstrate the significance of using the current approach for revealing brain-symptom relationships in patients with tauopathy. The observations indicating specific remote effects of tau deposits on particular symptoms is consistent with the notion that cortical dysfunctions in patients with PSP, including the frontal cognitive deficits, do not result directly from local tau deposits, but rather stem from network disruption that are remotely triggered by subcortical tau accumulation[20,22]. Although the current use of tau-network mapping itself did not specifically focus on cognitive deficits, the resultant strength of the FC between tau-deposition sites and the derived PSP-tau network specifically explained several frontal cognitive aspects of the clinical scores, rather than the more general severity of the disease measured by the total

score of PSPRS or general cognitive abilities indexed by MMSE. This is likely because the majority of the derived PSP-tau network comprised regions of the frontal cortex. The total PSPRS score was instead directly correlated with the degree of atrophy in the midbrain and cerebellum, which was consistent with previous studies[43].

Tau deposits were not located entirely heterogeneously across patients, but were partially overlapped, especially in the GP and midbrain. Indeed, these regions have been shown to exhibit significant positive FC and direct/indirect anatomical connectivity with some regions of the derived PSP-tau network[20,44]. This might raise a concern that the cortical pattern observed in the PSP-tau network is merely the reflection of FC with a specific primary region of tau deposit. However, correlations with clinical scores showed substantially different patterns between the amount of tau deposited in each of these regions and the strength of the FC from the tau-deposition sites to the PSP-tau network. This suggests that the derived PSP-tau network was not merely a simple reflection of the FC pattern from a specific single brain region showing highly overlapped tau depositions across patients, but instead presumably reflected the FCs from multiple nodes where tau deposits were distributed heterogeneously across patients.

While tau-network mapping revealed a prominent convergent network pattern, atrophy-network mapping for the same patients did not, across a range of statistical thresholds for defining seed regions. The results demonstrate the advantage of using tau deposits detected by florzolotau PET instead of atrophy captured by structural MRI to map the estimated effects of tau on remote brain regions and to clarify the brain-symptom relationships in PSP. Tau deposition itself should be toxic to neurons directly and indirectly, and thus would lead to neuronal dysfunctions even without atrophy. Note that atrophy-network mapping itself has been successfully conducted in previous studies including those for larger cohorts of patients with Alzheimer's disease[31] or schizophrenia[45]. In the current study, the local degree of both tau deposition and atrophy significantly explained motor-related symptoms with a similar sensitivity, denying the possibility that critical differences in data quality existed between the tau-deposition map and the atrophy map. However, we cannot rule out the possibility that more elaborated analysis of structural MRI data including normative modeling[46] with a larger cohort might improve the resultant atrophy-network map in the future.

Previous studies have shown significant changes in functional and anatomical connectivity in patients with PSP. In particular, cortico-subcortical changes in FC, including those between the midbrain/thalamus and cortical areas, have been reported[20,47]. Cortical targets of such changes in FC partially overlap with the currently identified PSP-tau network. Furthermore, significant hypoperfusion and hypometabolism have been

detected in the dACC, midcingulate cortex, and dlPFC of patients with PSP [24,48,49], which are close to some of the nodes of the PSP-tau network. Therefore, these physiological changes might at least be partially explained by the network we found in the present study based on the map of tau accumulation in individual patients.

The PSP-tau network largely overlapped with cingulo-opercular network (also known as action-mode network)[41,50]. This network is associated with planning, execution, monitoring, stopping of action, and attentional allocation based on both top-down regulation and bottom-up sensory input. In the present study, FC in individual patients between regions with tau deposits and the PSP-tau network were significantly anti-correlated with the total FAB score and its sub-scores, including a Go/NoGo task (Fig. 4), consistent with a role for the network in stopping planned actions. In particular, deficits in response inhibition is a primary symptom in PSP[51,52], and is likely reflected in the declined performance on a Go/NoGo task. Indeed, a majority of areas in the PSP-tau network are recruited by tasks requiring response inhibition[53], consistent with the currently observed relationships between the degree of suggested remote dysfunction of the PSP-tau network and the declined performance on a Go/NoGo task at the single-patient level.

The present study did not examine whether subcortical tau depositions cause actual dysfunction of the cortical PSP-tau network or whether dysfunction of PSP-tau network indeed leads to frontal cognitive symptoms. Recently, neural activity in nonhuman primates was able to be manipulated using chemogenetic techniques such as Designer Receptors Exclusively Activated by Designer Drugs (DREADDs) and Pharmacologically Selective Actuator Module / Pharmacologically Selective Effector Molecule (PSAM/PSEM) systems[54,55], and remote effects of neuronal silencing have been visualized at functionally connected regions with behavioral relevance[56,57]. Therefore, causal validation and mechanistic understanding of the results obtained with tau-network mapping via reverse translational interventions in non-human primate models is an intriguing direction for future research.

Other major limitations of the present study are as follows. First, although within-cohort reproducibility of the PSP-tau network was confirmed in a control analysis, its validation across independent cohorts would be required for more rigorous testing of reproducibility. Another limitation is the cross-sectional design of the research. Longitudinal study of the tau-PET and tracking changes in the PSP-tau network in association with the assessment of symptom progression would lead to a more causal understanding of the relationships between the PSP-tau-network and frontal cognitive symptoms. Another possibility for causal analysis is to test whether neuromodulation that

targets a node within the PSP-tau network can reduce frontal cognitive symptoms. If effective, it would represent a novel treatment option against PSP that relies on biological evidence.

The present study demonstrated that the tau-network mapping was able to identify a common cortical network to which tau deposition sites across PSP patients are functionally connected. Tau-PET images obtained from patients with PSP can thus be applied to identify the relationships linking the predominantly subcortical tau deposits, the remote dysfunction of the connected cortical networks, and the resultant frontal cognitive symptoms in individual patients with the aid of normative connectomes. The current approach provides a potential target for symptom-specific neuromodulatory treatment for patients with PSP, and might inform the future risk of frontal cognitive decline for patients in the early phase of the disease, based on still subthreshold amounts of tau deposits at brain regions connected to the PSP-tau network. Furthermore, this approach would be also widely appliable to other tauopathies including traumatic brain injury[58], late-onset psychiatric disorders, and Alzheimer's disease, for which tau deposits can be detected with florzolotau, as well as for other proteinopathies such as α-synucleinopathies[59], or other PET ligands measuring synaptic density or inflammation, to understand the mediating networks between the PET-detectable local structural/functional changes and the resultant symptoms in a range of brain diseases.

MATERIALS AND METHODS

Participants

Forty-six patients with PSP-Richardson syndrome (PSP-RS) and 50 healthy controls (HCs) aged older than 40 years, without histories of neurological disorders were recruited from our affiliated hospitals and the volunteer association of our institute, respectively. Patient details were described in our previous paper[37], but PSP participants with PSP-tau scores[37] less than 0.3 and HCs with PSP-tau scores more than 0.1 were excluded from the later analyses. The final number of participants included were 37 patients and 48 HCs. The participants underwent several neurological examinations, including the PSPRS, FAB, MMSE, Apathy Scale, and GDS.

PET and MRI data acquisition and preprocessing

Florzolotau PET images were acquired to detect tau deposits using a Biograph mCT flow system (Siemens, Erlangen, Germany) with 2 mm isotropic voxels. T1-weighted images (T1w) were acquired using a 3T MRI scanner (MAGNETOM Verio, Siemens, Erlangen, Germany) for registration of PET images to the standard MRI space and evaluating atrophy (repetition time [TR] = 2300 ms; echo time [TE] = 1.95 ms; inversion time [TI] = 900 ms; flip angle = 9°; field of view [FOV] = 250 mm; matrix size = 512 × 512 × 176; slice thickness = 1 mm). Detailed preprocessing was described in our previous paper[37]. Briefly, standardized uptake value ratio (SUVR) images were generated from averaged PET images for each participant with motion correction at the intervals of 90–110 min after intravenous injection of ^{18}F-florzolotau (186 ± 8.4 [MBq]). Individual SUVR images were spatially normalized to the standard Montreal Neurological Institute (MNI) space (East Asian brain T1w image from the International Consortium for Brain Mapping) using the Diffeomorphic Anatomical Registration Through Exponentiated Lie Algebra (DARTEL) algorithm from Statistical Parametric Mapping (SPM12, Wellcome Department of Cognitive Neurology), running on MATLAB (MathWorks).

Tau-network mapping

Tau-network mapping is an approach based on lesion-network mapping that identifies brain regions functionally connected to lesion locations. It does not use rs-fMRI scans of the participants themselves, but instead uses a large-scale open database of rs-fMRI acquired from healthy individuals. In this study, FC maps were computed using rs-fMRI data obtained from 100 healthy participants[25] from the Brain Genomics Superstruct Project (GSP)[38] with the locations of tau deposits in individual patients as seed regions. Figure S1 shows the analytical pipeline for tau-network mapping. In the first step, the

regions of tau deposits for each patient were identified by comparisons with tau PET images of healthy controls. The *t*-score maps for individual patients were thresholded at $p < 0.001$ (two-sided, uncorrected), and were binarized to create the volumes of interest (VOIs) for calculating FC maps. Next, the mean timeseries from the tau-deposit locations (i.e., VOIs) of a given patient for rs-fMRI data of each participant were compared with the timeseries from every voxel to calculate the correlation map. The maps for all 100 rs-fMRI datasets were then combined to calculate the *t*-score map for each patient. These maps for all 100 rs-fMRI datasets were combined to calculate the *t*-score map for each PSP patient. As a control condition of tau-network mapping, we also calculated *t*-score maps using pseudo-randomized VOIs. Briefly, ten voxels for each patient (total 370 voxels) were randomly selected in the brain. *t*-score maps were then calculated using these pseudo randomized VOIs in the same manner as the original *t*-score maps for tau deposits. Finally, random control-subtracted tau-derived FC map was obtained by contrasting between the FC maps derived from tau deposits and the randomized seeds. FC map calculation, statistical tests, and surface mapping were performed using FMRIB Software Library's (FSL's) FEAT tool[60], Analysis of Functional NeuroImages (AFNI) software[61], and Connectome Workbentch[62], respectively.

Atrophy-network mapping

Data preprocessing for VBM was performed using SPM12 on MATLAB and PMOD 4.2 / 4.3 (PMOD Technologies LLC, Switzerland). Gray and white matter segmentation images were extracted from T1w images and combined to obtain the parenchymal image using SPM12. The DARTEL algorithm was then employed to spatially normalize each brain parenchymal image (gray and white matter) by preserving amounts in MNI space. The regions of atrophy for each patient were identified by comparisons with parenchymal images of healthy controls. The *t*-score maps for each patient were thresholded at $p < 0.001$ (two-sided, uncorrected), and were binarized to create the VOIs for calculating FC maps. Later analyses were the same as those for the tau-network mapping described above.

Assignments of canonical networks to the derived PSP-tau network

Based on the atlas created by Ji et al.[40], one of twelve canonical networks including the orbito-affective, ventral multimodal, posterior multimodal, default mode, auditory, frontoparietal, language, dorsal attention, cingulo-opercular (action-mode[41]), somatomotor, and primary and secondary visual networks was assigned to each brain area in the derived PSP-tau network that was determined as a significant ($p < 0.05$, FWE-corrected) region in a statistical comparison (paired *t*-test) between the FC maps derived

from tau- and atrophy-network mapping among the patients. The proportion of each network among 38 areas in the PSP-tau network was then calculated and its unevenness was statistically evaluated using a Chi-square test.

Validation analyses of tau/atrophy-network mapping

To determine the seed region for tau/atrophy-network mapping, a statistical threshold of $p < 0.001$ (uncorrected) was adopted to identify the locations of significant tau deposition or atrophy in the patients compared with the healthy controls. To examine the consistency/stability of the tau/atrophy-network mapping results among different criteria for the seed definition, both more liberal ($p < 0.005$ uncorrected) and more stringent ($p < 0.05$ FWE) thresholds were also tested to identify the locations of tau deposition or atrophy in the patients for subsequent network mapping. To confirm the reproducibility of tau/atrophy network mapping in the current cohort of patients, tau-network maps calculated for individual patients (N = 37) were randomly divided into two groups, and the tau-network mapping was performed for these two groups separately. Then, the resultant FC values (with the tau deposition sites) in the Johns Hopkins University (JHU) whole brain VOIs were compared between the two groups. To confirm the consistency of tau-network mapping results among different rs-fMRI databases, we also performed tau-network mapping based on the Human Connectome Project (HCP)[39] data. For each patient, the FC map seeded from the tau-deposition sites was calculated with the HCP young adult dataset (N = 98) in the same manner as the analysis using the GSP dataset described above. The voxels with top 10% FC values in the cortex were then extracted from the resultant tau-network maps based on GSP/HCP data for comparison between the two rs-fMRI datasets.

Across-patient correlation between clinical scores and FC values linking tau deposits with the PSP-tau network

To visualize the regions whose strength of FC with tau-deposit sites explained the frontal cognitive impairments but not the motor-related dysfunction, we contrasted the correlation map between the FC and the frontal cognitive symptoms against that between the FC and motor deficits. Total FAB score and limb deficit score from the PSPRS were used as indices representing frontal cognitive and motor impairments, respectively. To assess the relationships between the clinical scores and the FC value (between the tau-deposition sites and each area in the PSP-tau network), we extracted the mean FC values (t-scores) in the whole PSP-tau network and its constituent seven clusters. These clusters were named adlPFC, PMC, IFC, dACC, Pre SMA, PPC, and AI based on a previous

human cortical parcellation[63]. We also extracted the amounts of tau deposition and atrophy (*t*-scores as described above) in the top two regions, i.e., the GP and midbrain for tau deposition and the midbrain and cerebellum for atrophy. Pearson's correlation coefficients were then calculated between these values and clinical scores (PSPRS and FAB). If a given index (i.e., the amount of tau/atrophy or the strength of FC) significantly correlated with PSPRS or FAB, then its sub-scores were also tested for correlation. Sub-scores which did not show significant correlation with any of the indices were not included in further analysis. The rest of the clinical scores (i.e., MMSE, Apathy Scale, and GDS) served as controls. Finally, the clinical scores with the strongest correlation were assigned to each brain region of the PSP-tau network. These analyses were performed using SPM12, Connectome Workbench, and FSL software.

References and Notes

1 Steele, J. C., Richardson, J. C. & Olszewski, J. Progressive Supranuclear Palsy. A Heterogeneous Degeneration Involving the Brain Stem, Basal Ganglia and Cerebellum with Vertical Gaze and Pseudobulbar Palsy, Nuchal Dystonia and Dementia. *Arch Neurol* **10**, 333-359 (1964). https://doi.org/10.1001/archneur.1964.00460160003001

2 Hauw, J. J. *et al.* Preliminary NINDS neuropathologic criteria for Steele-Richardson-Olszewski syndrome (progressive supranuclear palsy). *Neurology* **44**, 2015-2019 (1994). https://doi.org/10.1212/wnl.44.11.2015

3 Hoglinger, G. U. *et al.* Clinical diagnosis of progressive supranuclear palsy: The movement disorder society criteria. *Mov Disord* **32**, 853-864 (2017). https://doi.org/10.1002/mds.26987

4 Dubois, B., Slachevsky, A., Litvan, I. & Pillon, B. The FAB: a Frontal Assessment Battery at bedside. *Neurology* **55**, 1621-1626 (2000). https://doi.org/10.1212/wnl.55.11.1621

5 Donker Kaat, L. *et al.* Frontal presentation in progressive supranuclear palsy. *Neurology* **69**, 723-729 (2007). https://doi.org/10.1212/01.wnl.0000267643.24870.26

6 Ballatore, C., Lee, V. M. & Trojanowski, J. Q. Tau-mediated neurodegeneration in Alzheimer's disease and related disorders. *Nat Rev Neurosci* **8**, 663-672 (2007). https://doi.org/10.1038/nrn2194

7 Maruyama, M. *et al.* Imaging of tau pathology in a tauopathy mouse model and in Alzheimer patients compared to normal controls. *Neuron* **79**, 1094-1108 (2013). https://doi.org/10.1016/j.neuron.2013.07.037

8 Verny, M., Duyckaerts, C., Agid, Y. & Hauw, J. J. The significance of cortical pathology in progressive supranuclear palsy. Clinico-pathological data in 10 cases. *Brain* **119 (Pt 4)**, 1123-1136 (1996). https://doi.org/10.1093/brain/119.4.1123

9 Alster, P. *et al.* Accumulation of Tau Protein, Metabolism and Perfusion-Application and Efficacy of Positron Emission Tomography (PET) and Single Photon Emission Computed Tomography (SPECT) Imaging in the Examination of Progressive Supranuclear Palsy (PSP) and Corticobasal Syndrome (CBS). *Front Neurol* **10**, 101 (2019). https://doi.org/10.3389/fneur.2019.00101

10 Hauw, J. J. *et al.* Constant neurofibrillary changes in the neocortex in progressive supranuclear palsy. Basic differences with Alzheimer's disease and aging. *Neurosci Lett* **119**, 182-186 (1990). https://doi.org/10.1016/0304-3940(90)90829-x

11 Chen, Y. *et al.* Pathology-specific patterns of cerebellar atrophy in neurodegenerative disorders. *Alzheimers Dement* **20**, 1771-1783 (2024). https://doi.org/10.1002/alz.13551

12 Price, S. *et al.* Voxel-based morphometry detects patterns of atrophy that help differentiate progressive supranuclear palsy and Parkinson's disease. *Neuroimage* **23**, 663-669 (2004). https://doi.org/10.1016/j.neuroimage.2004.06.013

13 Josephs, K. A. *et al.* Voxel-based morphometry in autopsy proven PSP and CBD. *Neurobiol Aging* **29**, 280-289 (2008). https://doi.org/10.1016/j.neurobiolaging.2006.09.019

14 Boxer, A. L. *et al.* Patterns of brain atrophy that differentiate corticobasal degeneration syndrome from progressive supranuclear palsy. *Arch Neurol* **63**, 81-86 (2006). https://doi.org/10.1001/archneur.63.1.81

15 Cope, T. E. *et al.* Tau burden and the functional connectome in Alzheimer's disease and progressive supranuclear palsy. *Brain* **141**, 550-567 (2018). https://doi.org/10.1093/brain/awx347

16 Seeley, W. W., Crawford, R. K., Zhou, J., Miller, B. L. & Greicius, M. D. Neurodegenerative diseases target large-scale human brain networks. *Neuron* **62**, 42-52 (2009). https://doi.org/10.1016/j.neuron.2009.03.024

17 Seeley, W. W. *et al.* Early frontotemporal dementia targets neurons unique to apes and humans. *Ann Neurol* **60**, 660-667 (2006). https://doi.org/10.1002/ana.21055

18 Graveland, G. A., Williams, R. S. & DiFiglia, M. Evidence for degenerative and regenerative changes in neostriatal spiny neurons in Huntington's disease. *Science* **227**, 770-773 (1985). https://doi.org/10.1126/science.3155875

19 Selkoe, D. J. Alzheimer's disease is a synaptic failure. *Science* **298**, 789-791 (2002). https://doi.org/10.1126/science.1074069

20 Gardner, R. C. *et al.* Intrinsic connectivity network disruption in progressive supranuclear palsy. *Ann Neurol* **73**, 603-616 (2013). https://doi.org/10.1002/ana.23844

21 Gurd, J. M. & Hodges, J. R. Word-retrieval in two cases of progressive supranuclear palsy. *Behav Neurol* **10**, 31-41 (1997). https://doi.org/10.3233/BEN-1997-10106

22 Roemer, S. N. *et al.* Subcortical tau is linked to hypoperfusion in connected cortical regions in 4-repeat tauopathies. *Brain* **147**, 2428-2439 (2024). https://doi.org/10.1093/brain/awae174

23 Whitwell, J. L. *et al.* Radiological biomarkers for diagnosis in PSP: Where are we and where do we need to be? *Mov Disord* **32**, 955-971 (2017). https://doi.org/10.1002/mds.27038

24 Salmon, E., Van der Linden, M. V. & Franck, G. Anterior cingulate and motor network metabolic impairment in progressive supranuclear palsy. *Neuroimage* **5**, 173-178 (1997). https://doi.org/10.1006/nimg.1997.0262

25 Boes, A. D. *et al.* Network localization of neurological symptoms from focal brain lesions. *Brain* **138**, 3061-3075 (2015). https://doi.org/10.1093/brain/awv228

26 Darby, R. R., Laganiere, S., Pascual-Leone, A., Prasad, S. & Fox, M. D. Finding the imposter: brain connectivity of lesions causing delusional misidentifications. *Brain* **140**, 497-507 (2017). https://doi.org/10.1093/brain/aww288

27 Ferguson, M. A. *et al.* A human memory circuit derived from brain lesions causing amnesia. *Nat Commun* **10**, 3497 (2019). https://doi.org/10.1038/s41467-019-11353-z

28 Fischer, D. B. *et al.* A human brain network derived from coma-causing brainstem lesions. *Neurology* **87**, 2427-2434 (2016). https://doi.org/10.1212/WNL.0000000000003404

29 Darby, R. R., Horn, A., Cushman, F. & Fox, M. D. Lesion network localization of criminal behavior. *Proc Natl Acad Sci U S A* **115**, 601-606 (2018). https://doi.org/10.1073/pnas.1706587115

30 Laganiere, S., Boes, A. D. & Fox, M. D. Network localization of hemichorea-hemiballismus. *Neurology* **86**, 2187-2195 (2016). https://doi.org/10.1212/WNL.0000000000002741

31 Tetreault, A. M. *et al.* Network localization of clinical, cognitive, and neuropsychiatric symptoms in Alzheimer's disease. *Brain* **143**, 1249-1260 (2020). https://doi.org/10.1093/brain/awaa058

32 Padmanabhan, J. L. *et al.* A Human Depression Circuit Derived From Focal Brain Lesions. *Biol Psychiatry* **86**, 749-758 (2019). https://doi.org/10.1016/j.biopsych.2019.07.023

33 Joutsa, J. *et al.* Brain lesions disrupting addiction map to a common human brain circuit. *Nat Med* **28**, 1249-1255 (2022). https://doi.org/10.1038/s41591-022-01834-y

34 Luan, Y. *et al.* Tau-network mapping of domain-specific cognitive impairment in Alzheimer's disease. *Neuroimage Clin* **44**, 103699 (2024). https://doi.org/10.1016/j.nicl.2024.103699

35 Tagai, K. *et al.* High-Contrast In Vivo Imaging of Tau Pathologies in Alzheimer's and Non-Alzheimer's Disease Tauopathies. *Neuron* **109**, 42-58 e48 (2021). https://doi.org/10.1016/j.neuron.2020.09.042

36 Tezuka, T. *et al.* Evaluation of [(18)F]PI-2620, a second-generation selective tau tracer, for assessing four-repeat tauopathies. *Brain Commun* **3**, fcab190 (2021). https://doi.org/10.1093/braincomms/fcab190

37 Endo, H. *et al.* A Machine Learning-Based Approach to Discrimination of Tauopathies Using [(18) F]PM-PBB3 PET Images. *Mov Disord* **37**, 2236-2246 (2022). https://doi.org/10.1002/mds.29173

38 Yeo, B. T. *et al.* The organization of the human cerebral cortex estimated by intrinsic functional connectivity. *J Neurophysiol* **106**, 1125-1165 (2011). https://doi.org/10.1152/jn.00338.2011

39 Van Essen, D. C. *et al.* The WU-Minn Human Connectome Project: an overview. *Neuroimage* **80**, 62-79 (2013). https://doi.org/10.1016/j.neuroimage.2013.05.041

40 Ji, J. L. *et al.* Mapping the human brain's cortical-subcortical functional network organization. *Neuroimage* **185**, 35-57 (2019). https://doi.org/10.1016/j.neuroimage.2018.10.006

41 Dosenbach, N. U. F., Raichle, M. E. & Gordon, E. M. The brain's action-mode network. *Nat Rev Neurosci* (2025). https://doi.org/10.1038/s41583-024-00895-x

42 Siddiqi, S. H., Kording, K. P., Parvizi, J. & Fox, M. D. Causal mapping of human brain function. *Nat Rev Neurosci* **23**, 361-375 (2022). https://doi.org/10.1038/s41583-022-00583-8

43 Dutt, S. *et al.* Progression of brain atrophy in PSP and CBS over 6 months and 1 year. *Neurology* **87**, 2016-2025 (2016). https://doi.org/10.1212/WNL.0000000000003305

44 Middleton, F. A. & Strick, P. L. Anatomical evidence for cerebellar and basal ganglia involvement in higher cognitive function. *Science* **266**, 458-461 (1994). https://doi.org/10.1126/science.7939688

45 Makhlouf, A. T. *et al.* Heterogeneous patterns of brain atrophy in schizophrenia localize to a common brain network. *Nature Mental Health* (2024). https://doi.org/https://doi.org/10.1038/s44220-024-00348-5

46 Segal, A. *et al.* Regional, circuit and network heterogeneity of brain abnormalities in psychiatric disorders. *Nat Neurosci* **26**, 1613-1629 (2023). https://doi.org/10.1038/s41593-023-01404-6

47 Piattella, M. C. *et al.* Disrupted resting-state functional connectivity in progressive supranuclear palsy. *AJNR Am J Neuroradiol* **36**, 915-921 (2015). https://doi.org/10.3174/ajnr.A4229

48 Chiu, W. Z. *et al.* Midcingulate involvement in progressive supranuclear palsy and tau positive frontotemporal dementia. *J Neurol Neurosurg Psychiatry* **83**, 910-915 (2012). https://doi.org/10.1136/jnnp-2011-302035

49 Varrone, A. *et al.* Identification by [99mTc]ECD SPECT of anterior cingulate hypoperfusion in progressive supranuclear palsy, in comparison with Parkinson's

disease. *Eur J Nucl Med Mol Imaging* **34**, 1071-1081 (2007). https://doi.org/10.1007/s00259-006-0344-7

50 Dosenbach, N. U. *et al.* A core system for the implementation of task sets. *Neuron* **50**, 799-812 (2006). https://doi.org/10.1016/j.neuron.2006.04.031

51 Zhang, J. *et al.* Different decision deficits impair response inhibition in progressive supranuclear palsy and Parkinson's disease. *Brain* **139**, 161-173 (2016). https://doi.org/10.1093/brain/awv331

52 Migliaccio, R. *et al.* Cognitive and behavioural inhibition deficits in neurodegenerative dementias. *Cortex* **131**, 265-283 (2020). https://doi.org/10.1016/j.cortex.2020.08.001

53 Aron, A. R. & Poldrack, R. A. Cortical and subcortical contributions to Stop signal response inhibition: role of the subthalamic nucleus. *J Neurosci* **26**, 2424-2433 (2006). https://doi.org/10.1523/JNEUROSCI.4682-05.2006

54 Nagai, Y. *et al.* Deschloroclozapine, a potent and selective chemogenetic actuator enables rapid neuronal and behavioral modulations in mice and monkeys. *Nat Neurosci* **23**, 1157-1167 (2020). https://doi.org/10.1038/s41593-020-0661-3

55 Hori, Y. *et al.* Multimodal Imaging for Validation and Optimization of Ion Channel-Based Chemogenetics in Nonhuman Primates. *J Neurosci* **43**, 6619-6627 (2023). https://doi.org/10.1523/JNEUROSCI.0625-23.2023

56 Hirabayashi, T. *et al.* Chemogenetic sensory fMRI reveals behaviorally relevant bidirectional changes in primate somatosensory network. *Neuron* **109**, 3312-3322 e3315 (2021). https://doi.org/10.1016/j.neuron.2021.08.032

57 Hirabayashi, T. *et al.* Multiscale Chemogenetic Dissection of Fronto-temporal Top-down Regulation for Object Memory in Primates. *Nature Communications* (2024). https://doi.org/https://doi.org/10.1038/s41467-024-49570-w

58 Takahata, K. *et al.* PET-detectable tau pathology correlates with long-term neuropsychiatric outcomes in patients with traumatic brain injury. *Brain* **142**, 3265-3279 (2019). https://doi.org/10.1093/brain/awz238

59 Endo, H. *et al.* Imaging alpha-synuclein pathologies in animal models and patients with Parkinson's and related diseases. *Neuron* **112**, 2540-2557 e2548 (2024). https://doi.org/10.1016/j.neuron.2024.05.006

60 Smith, S. M. *et al.* Advances in functional and structural MR image analysis and implementation as FSL. *Neuroimage* **23 Suppl 1**, S208-219 (2004). https://doi.org/10.1016/j.neuroimage.2004.07.051

61 Cox, R. W. AFNI: software for analysis and visualization of functional magnetic resonance neuroimages. *Comput Biomed Res* **29**, 162-173 (1996). https://doi.org/10.1006/cbmr.1996.0014

62 Marcus, D. S. *et al.* Informatics and data mining tools and strategies for the human connectome project. *Front Neuroinform* **5**, 4 (2011). https://doi.org/10.3389/fninf.2011.00004

63 Glasser, M. F. *et al.* A multi-modal parcellation of human cerebral cortex. *Nature* **536**, 171-178 (2016). https://doi.org/10.1038/nature18933

Acknowledgments:
We thank all patients and their caregivers, as well as volunteers, for their participation in this study; clinical research coordinators; PET and MRI operators; radiochemists; and research ethics advisers at Quantum Science and Technology (QST) for their assistance with the current projects. We acknowledge the support of Matsuoka, K. Hirata, M. Oya, H. Matsumoto, M. Ichihashi, Y. Komatsu, Y. Yamamoto, M. Kubota, K. S. Kitamura, Y. Takado, K. Kawamura, and M.R. Zhang at QST. We thank APRINOIA Therapeutics for kindly sharing the precursor of florzolotau (18F). We acknowledge the support of S. Hirano and Y. Nakano at the Department of Neurology, Chiba University on patient recruitment; T. Hatano, T. Tsunemi, N. Nishikawa, K. Nishioka (currently working at The Juntendo Tokyo Koto Geriatric Medical Center), Y. Yamashita, Y. Motoi, and S. Saiki (currently working at the University of Tsukuba) at the Department of Neurology, Juntendo University School of Medicine; I. Aiba at the Department of Neurology, National Hospital Organization Higashinagoya National Hospital; T. Yuasa at the Department of Neurology, Kamagaya General Hospital; H. Imai at the Tokyo Rinkai Hospital; Y. Nishida and Y. Yagi at the Department of Neurology, Tokyo Medical and Dental University; S. Furukawa at the Narita Red Cross Hospital; M. Seki at the Department of Neurology, Keio University School of Medicine; and T. Takeda and I. Isose at the Department of Neurology, Chiba-East Hospital. Data were provided in part by the Human Connectome Project, WU-Minn Consortium (Principal Investigators: David Van Essen and Kamil Ugurbil; 1U54MH091657) funded by the 16 NIH Institutes and Centers that support the NIH Blueprint for Neuroscience Research; and by the McDonnell Center for Systems Neuroscience at Washington University. We also thank Adam Phillips, PhD, from Edanz (https://jp.edanz.com/ac) for editing a draft of this manuscript.

Funding:
AMED Grant JP24wm0625307 (to TH)
AMED Grant JP19dm0207072 (to MH)
AMED Grant JP24wm0625001 (to MH)
JST Grant JPMJMS2024 (to MH)
MEXT/JSPS KAKENHI JP24H00734 (to TH)
MEXT/JSPS KAKENHI JP23K11796 (to YH)
Biogen Idec Inc.
APRINOIA Therapeutics.

Author contributions:

Conceptualization: TH
Methodology: YH, TH, HE
Investigation: YH, TH, HE
Visualization: YH, TH
Funding acquisition: TH, YH, HE, MH, TM
Project administration: TH
Supervision: TH, EH, TM, MH
Writing – original draft: YH, TH
Writing – review & editing: All authors

Competing interests:

H. Shimada, and M.H. hold patents on compounds related to this report.

Data and materials availability:

The data supporting our study findings are available from the corresponding author upon reasonable request.

Supplementary Figures

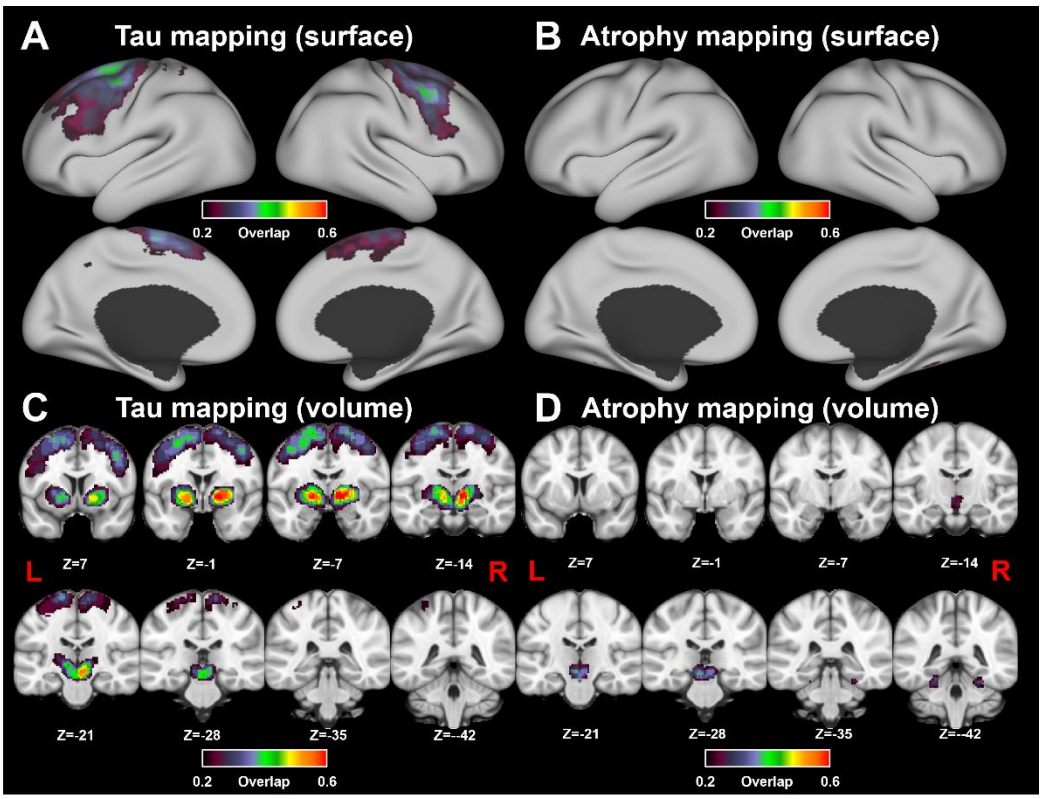

Fig. S1 Overlap of tau deposit and brain atrophy locations among patients with PSP. Overlap maps for tau deposit (A, C) and atrophy (B, D) are presented on the surface (A, B) and in volume space (C, D). Significant tau accumulation was observed in the GP (thresholded at $p < 0.001$, overlapped maximally for 62% of patients), thalamus (62%) and midbrain (57%), and parts of motor-related cortex (25%), while brain atrophy was significantly observed in the midbrain (35%) and cerebellum (32%).

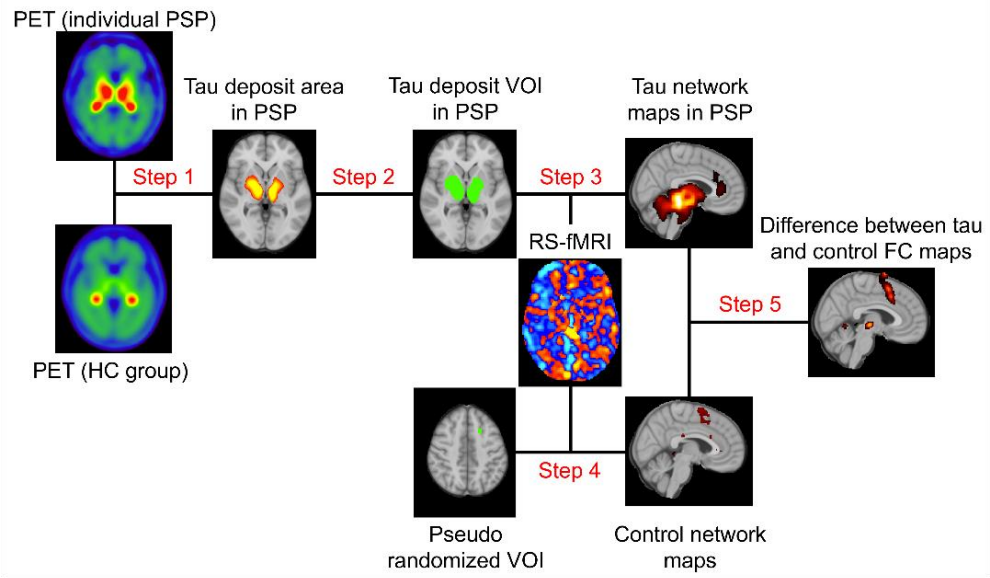

Fig. S2 Pipeline for tau network mapping. Tau deposition sites for each patient were identified by comparisons with tau PET images from healthy controls (Step 1). The *t*-score maps of tau deposition for individual patients were then thresholded at $p < 0.001$ (uncorrected), and binarized to create the VOIs (Step 2). Next, the mean timeseries in the VOI from each rs-fMRI data ($N = 100$) were compared with timeseries for every voxel to calculate the correlation maps (tau network maps). The maps for all 100 rs-fMRI datasets were combined to calculate the *t*-score maps for each patient (Step 3). As a control condition, ten voxels for each patient were generated by randomly selecting a position in the brain. *t*-score maps were calculated using pseudo randomized voxels in the same manner as using the tau deposit VOIs, as described above (Step 4) Finally, tau-derived FC map was obtained by calculating a differential *t*-score map between tau deposit and control FC maps (Step 5).

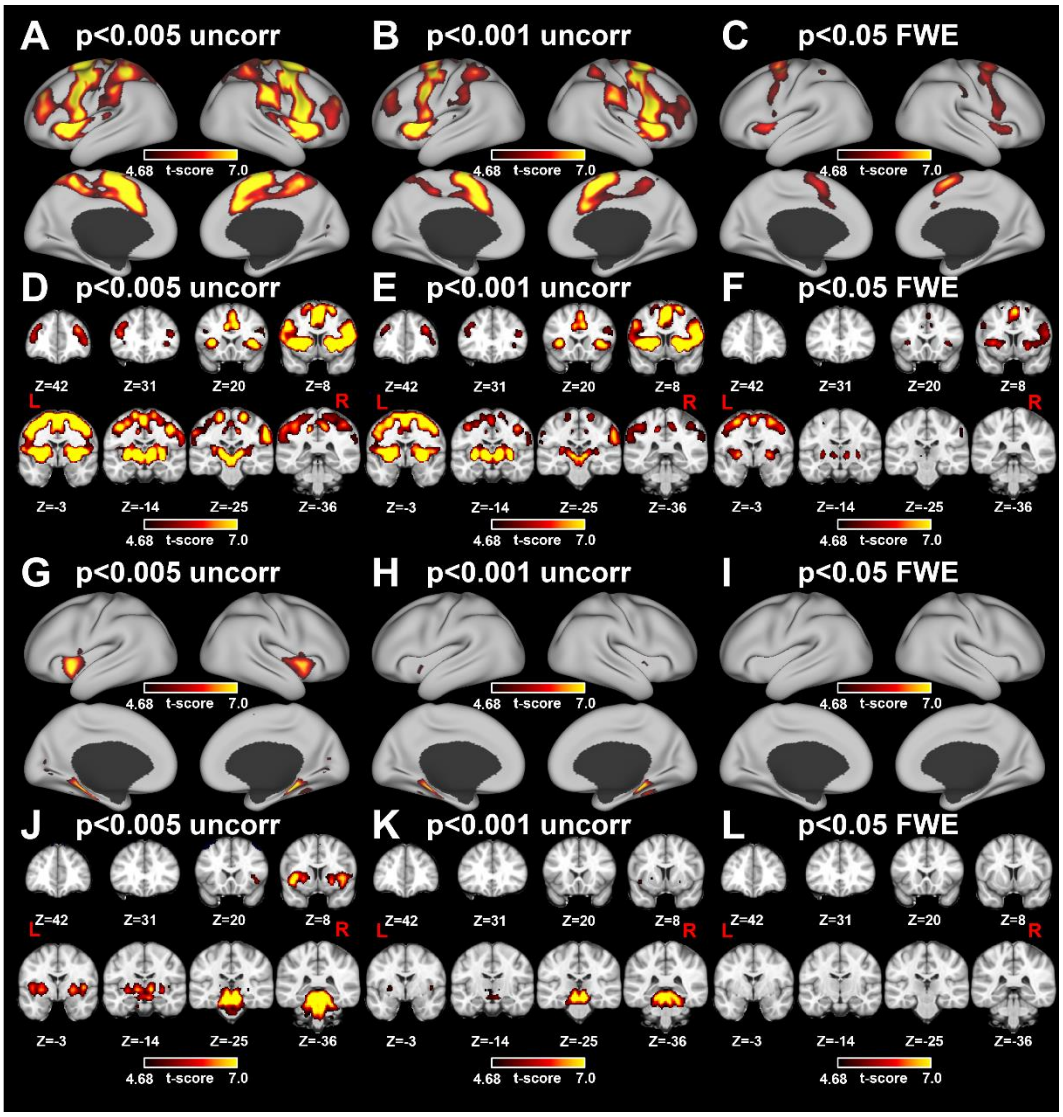

Fig. S3 Tau/atrophy network maps with different thresholds for seed definition. Tau (A-F) and atrophy (G-L) network maps were obtained using seed regions derived from tau deposits and atrophy with three different thresholds ($p < 0.005$ uncorrected, $p < 0.001$ uncorrected, and $p < 0.05$ FWE corrected).

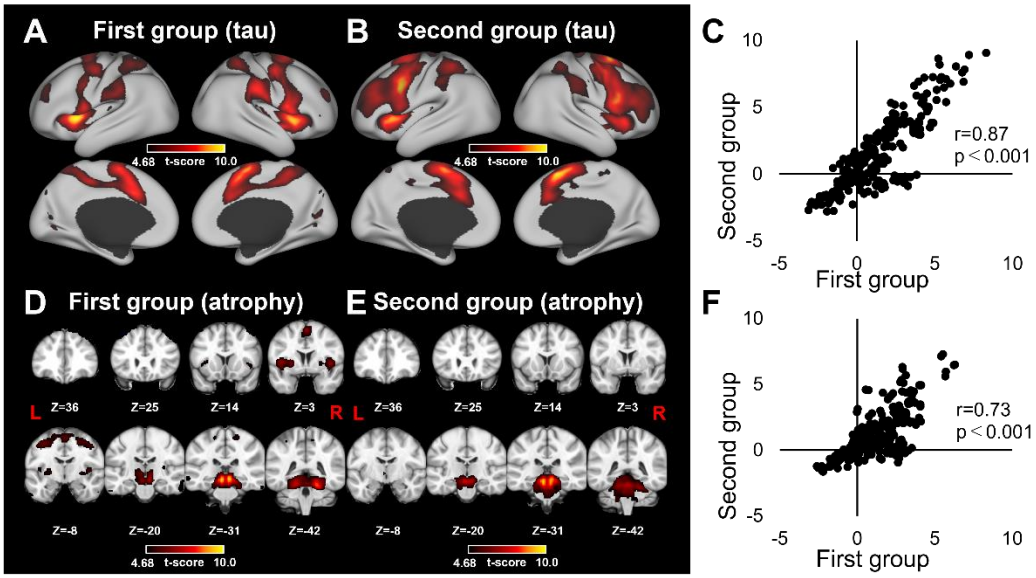

Fig. S4 Reproducibility of tau/atrophy-network mapping. **(A-C)** Comparisons of tau-network mapping results for split-half subgroups. Correlation of FC values for the same region was plotted in (C). **(D-E)** Same as (A-C), but for atrophy. Volume maps were adopted instead of surface maps for atrophy due to subcortical predominance. The VOI values in the tau/atrophy-network maps across the whole brain were highly consistent between the two groups of patients ($r = 0.87$ and 0.73, $p < 0.001$ for tau- and atrophy-network map, respectively).

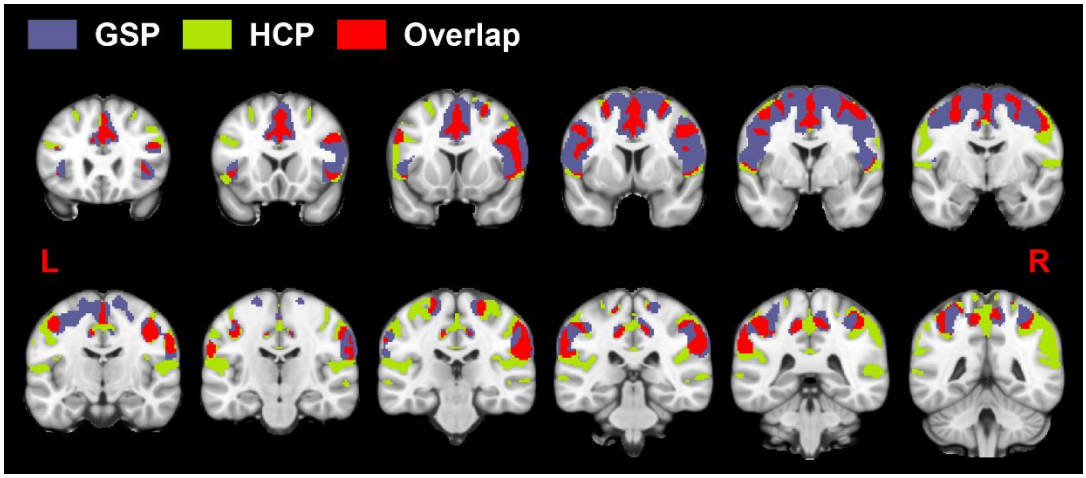

Fig. S5 Consistency of tau-network mapping results across two different rs-fMRI databases. Tau-network maps were computed based on GSP and HCP databases. Voxels showing top 10% of the FC values in the cortex are shown in blue and green for GSP and HCP, respectively. Overlap between the tau-network maps based on the two databases were depicted in red, including the LPFC, dACC, PPC, and AI.

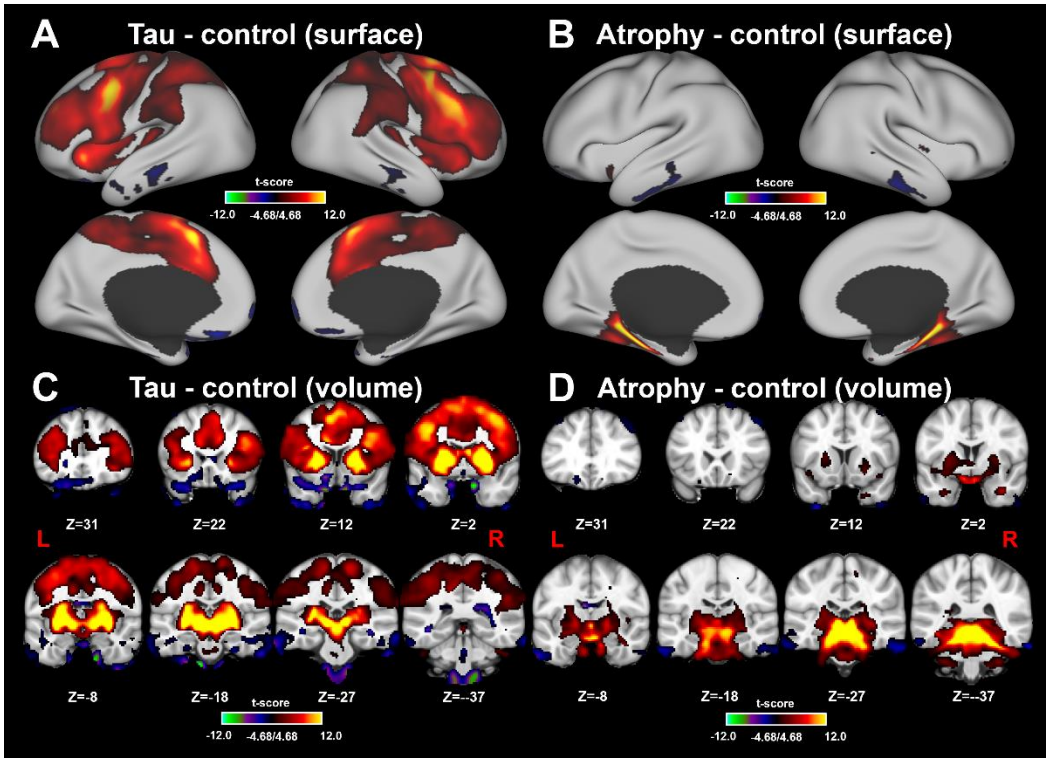

Fig. S6 Comparison of tau/atrophy-network maps with control FC maps calculated with pseudo-randomized seed regions. **(A, C)** Control-subtracted tau-network map presented in the surface (A) and volume (C) spaces, respectively. **(B, D)** Same as (A, C), but for atrophy-network mapping .

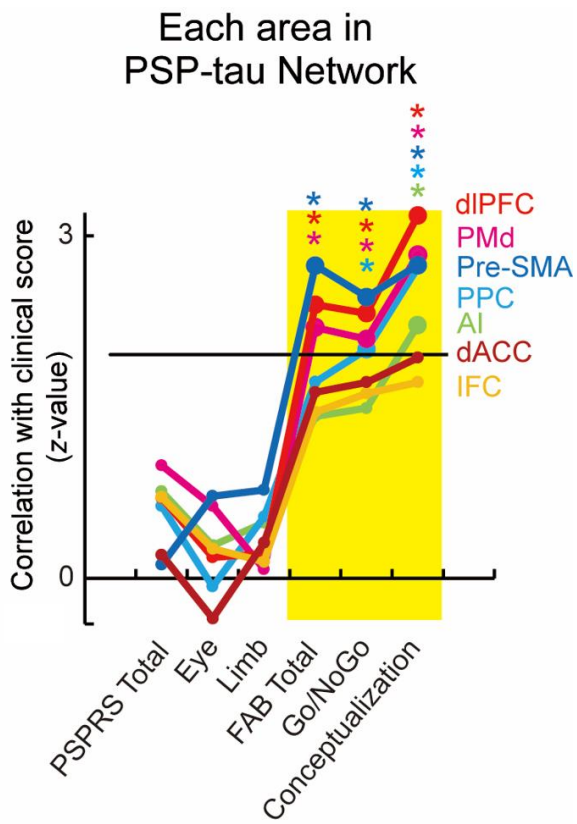

Fig. S7 Correlation between the FC from tau deposits to each area in the PSP-tau network and clinical symptom scores. Red, adlPFC; magenta, PMd; blue, Pre-SMA; cyan, PPC; light green, AI; brown, dACC; Yellow, IFC. Black horizontal line, statistical threshold (p = 0.05). *, significant correlation.

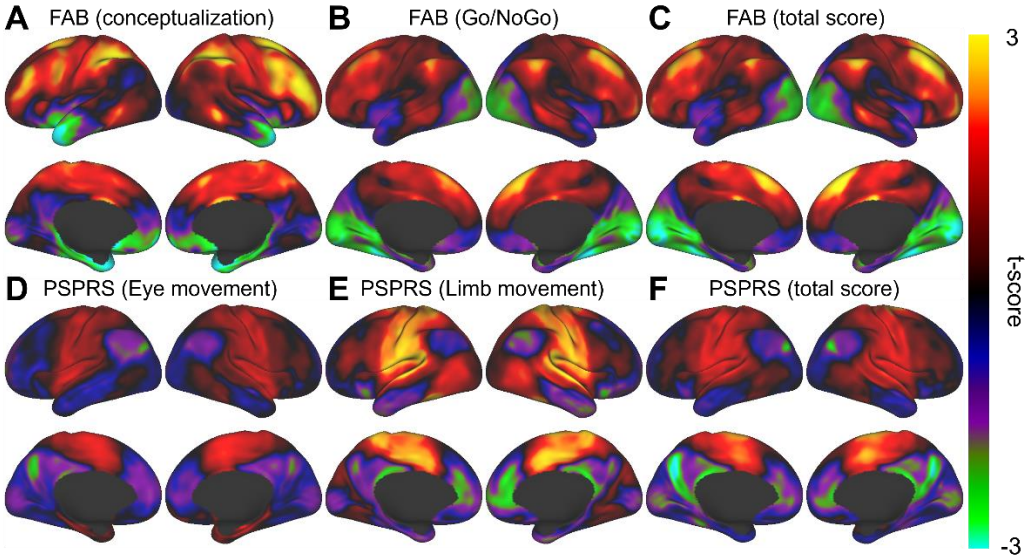

Fig. S8 Correlation maps between the FC value from tau deposition sites and the degree of cognitive (A-C) and motor (D-F) symptoms.